Reprinted from JOURNAL OF COMPUTATIONAL PHYSICS
Vol. 89, No. 1, July 1990
Printed in Belgium

Numerical Implementation of Relativistic Electromagnetic Boundary Conditions in a Laboratory-Frame Grid*

FADY HARFOUSH

Fermi National Accelerator Laboratory, Batavia, Illinois 60510

AND

ALLEN TAFLOVE AND GREGORY A. KRIEGSMANN

Northwestern University, Evanston, Illinois 60208

Received June 6, 1988; revised January 24, 1989

A new method for modeling moving, perfectly conducting surfaces is analyzed using a numerical technique based on the finite-difference time domain (FD-TD) method. Contrary to any other method, the numerical technique used does not require a system transformation where the object is at rest but gives a solution to the problem directly in the laboratory frame. The central idea of this new technique is the direct finite difference implementation of the relativistic boundary conditions at a moving surface. The electromagnetic wave scattering properties of a uniformly moving and vibrating rectangular cylinder are analyzed, first in one dimension and then in two dimensions. Results obtained are in excellent agreement with published analytical results. The new approach provides a method to analyze different problems of moving perfectly conducting scatterers where alternative analytical means are not available. Moreover, the time evolution of the fields are directly observable in the laboratory frame.

1. INTRODUCTION

The analysis of electromagnetic wave interactions with moving surfaces is of importance in studies of moving-target detection, generation of high-power microwave energy by moving dense plasmas, and astrophysical phenomena. Such problems can generally be divided in two categories: low-velocity effects (moving solid targets) and high-velocity effects (relativistic moving plasmas, astrophysics). Problems involving low velocities can be simplified by considering only first order terms in v/c (c being the velocity of light in free space). Problems involving relativistic velocities are more difficult to solve analytically and increasingly are being approached via numerical techniques.

In most cases, analytical approaches for the electrodynamics of moving bodies employ a system transformation wherein the object is at rest. Such a transformation is well defined for uniformly moving and is known as the Lorentz transformation [1].

* This work was supported in part by National Foundation Grant ASC-8811273 and office of Naval Research Contract N00014-88-K-0475.

0021-9991/90 $3.00

However, for non-uniform motion, a calculation using tensors is required to define a system where the object is relatively at rest [2]. Such calculations can become very complicated since the characteristics of the problem in the observer frame (field polarization, media parameters) are changed in the moving frame. Numerical simulation of such problems has followed the same pattern [3].

A direct way of approaching a moving-surface problem without using a system transformation involves the application of relativistic boundary conditions at the moving surface. For a moving material interface, these conditions are given by [4]:

$$\mathbf{n} \times (\mathbf{E}_2 - \mathbf{E}_1) - (\mathbf{n} \cdot \mathbf{v})(\mathbf{B}_2 - \mathbf{B}_1) = 0 \tag{1}$$

$$\mathbf{n} \cdot (\mathbf{B}_2 - \mathbf{B}_1) = 0. \tag{2}$$

$$\mathbf{n} \cdot (\mathbf{D}_2 - \mathbf{D}_1) = \rho_s \tag{3}$$

$$\mathbf{n} \times (\mathbf{H}_2 - \mathbf{H}_1) + (\mathbf{n} \cdot \mathbf{v})(\mathbf{D}_2 - \mathbf{D}_1) = \mathbf{J}_\mathbf{s}. \tag{4}$$

where $\mathbf{E_i}$, $\mathbf{D_i}$, $\mathbf{H_i}$, and $\mathbf{B_i}$ are, respectively, the electric field, electric flux density, magnetic field, and magnetic flux density in medium i; ρ_s and $\mathbf{J_s}$ denote the surface-charge and current densities; $\mathbf{v}$ is the velocity of the surface boundary (assumed to be uniform), and $\mathbf{n}$ is the unit vector normal to the surface.

Note that (1), (2), and the radiation condition provide the complete problem physics, assuming that we initially have no surface charge and current density. It is also important to note from (1), (4) that a scatterer motion transverse to the surface plane (perpendicular to the surface normal) results in boundary conditions similar to that of a fixed object, simply because the term $\mathbf{n} \cdot \mathbf{v}$ is now equal to 0. Further, (1) implies that the tangential E-field at the surface of a perfectly conducting moving boundary can be finite. However, this does not result in an infinite surface current density because the usual expression, $\mathbf{J} = \sigma\mathbf{E}$, for current density in a material of conductivity, σ, is no longer valid. Instead, for a uniformly moving object, the total induced current is the result of a conduction current plus a convection current. Defining β as the ratio v/c, c being the velocity of light in free space, the total current is given by

$$\mathbf{J} = \sigma(\mathbf{E} + \mathbf{v} \times \mathbf{B}) \frac{1}{\sqrt{1 - \beta^2}} \tag{5}$$

where, for a perfect conductor, $\mathbf{E} + \mathbf{v} \times \mathbf{B} = 0$ from (1); and therefore the surface current density $\mathbf{J_s}$ remains finite. In many references, only small velocities are considered and the term β^2 is neglected compared to 1.

In the derivation of the above equations, no assumption is made on the speed v relative to the speed of light c, hence the designation relativistic boundary conditions. The only assumption made is that the speed v is uniform. However, the same relativistic boundary conditions derived for uniform v have been widely applied to study accelerating bodies, under certain conditions where the acceleration is sufficiently low [5]. Here, a new reference frame called the "co-moving

frame" or "instantaneous frame" is introduced [2]. The difference is that now the velocity v in (1), (4) represents the instantaneous velocity instead of the uniform velocity. The term "Doppler approximation" [6] is also used to denote analyses wherein it is assumed that the instantaneous velocity equals a uniform velocity. It is not within the scope of this paper to discuss the details of this theory. Its validity in rotating coordinates has been investigated by Shiozawa [5]. The reader can also refer to the presentation given in [4, 2].

In this paper, we discuss a new numerical technique that appears novel in that it uses no system transformation. Instead it applies relativistic boundary conditions to provide the solution directly in the laboratory frame. It exploits the detailed modeling characteristics of the finite-difference time-domain (FD-TD) technique and has the potential to permit accurate numerical modeling of moving/vibrating rigid body problems of substantially more complexity than existing analytical approaches.

FD-TD is a direct solution of Maxwell's time-dependent curl equations using finite differences. Since its introduction [7–11], the method has been applied to a wide range of problems involving electromagnetic wave interactions with stationary two- and three-dimensional conducting, dielectric, and anisotropic structures. A recent review is given in [12]. Due to the time-domain nature of FD-TD, it is, in principle, applicable to direct modeling of wave interaction with time-varying surfaces. Our initial work in this area involved wave scattering from a half-space media having time-varying conductivity [13]. We subsequently considered wave scattering from relativistically moving perfectly conducting surfaces [14], using relativistic boundary conditions (1) in a laboratory frame grid. Boundary condition (1) relates the E field and H field linearly at the same point in space and time. This makes it impossible to implement in the FD-TD code, since there the E field and the H field are computed in a leapfrog manner at half-step intervals in time and space. It is therefore necessary to derive an equivalent form of (1) wherein implementation in the FD-TD code is possible. In [14], this derivation assumed that the reflected waves from the moving mirror act like plane waves. Such an assumption is exact for normal incidence and/or uniform motion but not for oblique incidence on a vibrating mirror. In this paper, we provide an improved model of relativistic motion which eliminates the need for such an assumption. The validity of this new method will be verified by considering again several cases of uniformly moving or vibrating infinite plane mirrors.

In the next section, we first briefly review the models used in [14] to numerically implement the required relativistic electromagnetic field boundary conditions. We then present an improved technique for achieving the same goal. Section 3 discusses validation studies for the uniformly moving and vibrating infinite mirror at normal incidence using the improved technique. Section 4 studies the case of a vibrating infinite mirror at oblique incidence again using the improved technique. Last, Section 5 provides the summary and conclusions.

2. Relativistic Boundary Conditions in an FD-TD Code

2.1. *Brief Description of the Earlier Methods*

2.1.1. *Quasi-stationary Method*

This is the most simple approach to model a moving boundary and is widely used analytically to obtain a first approximation of the reflected field [2, 6]. For a uniformly moving mirror, this method gives the proper shift in frequency but leaves the amplitude of the reflected field unchanged. For the vibrating mirror case, the method predicts the generation of sidebands having amplitudes proportional to a zero-order Bessel function, similar to an FM-tone modulation. The modeling of the quasi-stationary method in the FD-TD code is relatively simple, with the mirror actually moving in the grid. The total tangential E-field at the mirror surfaces satisfies the boundary condition of a stationary perfectly conducting surface, i.e., is set equal to zero. Similarly, the total tangential H-field at the mirror surface is set equal to twice the incident H field. To compute the E and H fields next to the mirror surface, we use a contour integral model [14, 15].

2.1.2. *Semi-relativistic Method*

This method utilizes an equivalent relativistic boundary condition for the total tangential E or H field at the moving boundary surface based on the plane-wave assumption discussed earlier. In [14], the electric field is selected. This yields an equivalent relativistic boundary condition that relates the total tangential E field at the moving surface to the incident tangential E field. A contour integral model is used to compute the H field adjacent to the moving surface. Reference [14] shows that this model provides excellent agreement with published analytical results for scattered fields generated by an infinite conducting surface undergoing uniform translation or vibration. For the vibration cases considered, the dominant propagating modes act together almost like a plane wave, fulfilling the basic assumption of the model.

2.1.3. *Fully-relativistic Method*

This approach is similar to the semi-relativistic method except that now the equivalent relativistic boundary condition is implemented for both the E and the H fields. This approach is actually simpler to implement than the semi-relativistic model because it does not require a contour integral. Again, Reference [14] shows excellent agreement of the model with published analytical results.

2.2. *The Improved Model*

We now propose a new, more robust approach, where the plane-wave assumption used in our earlier models is removed. This permits accurate modeling of more general relativistic motion by arbitrary conducting bodies where it is not

clear a priori that the combined action of the dominant propagating modes approximates a plane wave. In this new model, we attempt to directly implement condition (1) and (2). In using (1) to calculate the tangential E field at the moving surface, there is no restriction on the time-varying velocity. However, a potential singularity problem arises when using (1) to calculate the tangential H field at the moving surface, since now v shows up in the denominator and may equal zero at particular times. We need an alternate relation for the tangential H field that does not have the singularity problem at $v=0$. Starting from (1), it is possible to derive such a relation that is suitable for FD-TD implementation at the moving object surface. Details of the derivation are given in the Appendix. The result is

$$\mu \frac{dH}{dt} = \frac{(v^2 - c^2)}{(v^2 + c^2)} \cdot \frac{\partial E}{\partial y} - \frac{1}{(v^2 + c^2)} \cdot \frac{dv}{dt} \cdot E, \tag{6}$$

where μ is the free space permittivity and E and H represent the total tangential electric and magnetic fields, respectively, at the moving boundary surface. At $v=0$, (6) reduces to a form identical to Maxwell's curl E equation, clearly with no singularities. Equation (6) is suitable for the FD-TD algorithm because it can be computed every time step in parallel with H field computation. Note that because the E field has a step change from a non-zero value at the moving object surface to a zero value inside the perfectly conducting object, the partial space derivative in (6) represents a one-sided derivative.

Our new model thus consists of condition (1) applied to the moving-surface total tangential E field, (2) applied to the moving-surface total normal H field, and (6) applied to the moving-surface total tangential H field. By finite-differencing (1), we obtain

$$E_m^n = v^n \cdot \mu \cdot H_m^n, \tag{7}$$

where the subscript m denotes a total tangential field value exactly at the object surface and the surface H-field value at time n is computed by linearly extrapolating the H-field values at times $n-1/2$ and $n-3/2$ as follows:

$$H_m^n = 1.5 \cdot H_m^{n-1/2} - 0.5 \cdot H_m^{n-3/2}. \tag{8}$$

Condition (2) yields

$$H_{\text{normal}}^n = 0 \qquad \text{for all} \quad n. \tag{9}$$

Finally, for (6), we obtain

$$\mu \frac{H_m^{n+1/2} - H_m^{n-1/2}}{dt} = \frac{(v^2 - c^2)}{(v^2 + c^2)} \cdot \frac{E_m^n - E^n}{dy'} - \frac{1}{(v^2 + c^2)} \cdot \frac{dv}{dt} \cdot E_m^n. \tag{10}$$

Here, the symbol E with no subscript denotes the non-zero total tangential electric field value at the grid point adjacent to the object surface, and dy' is the

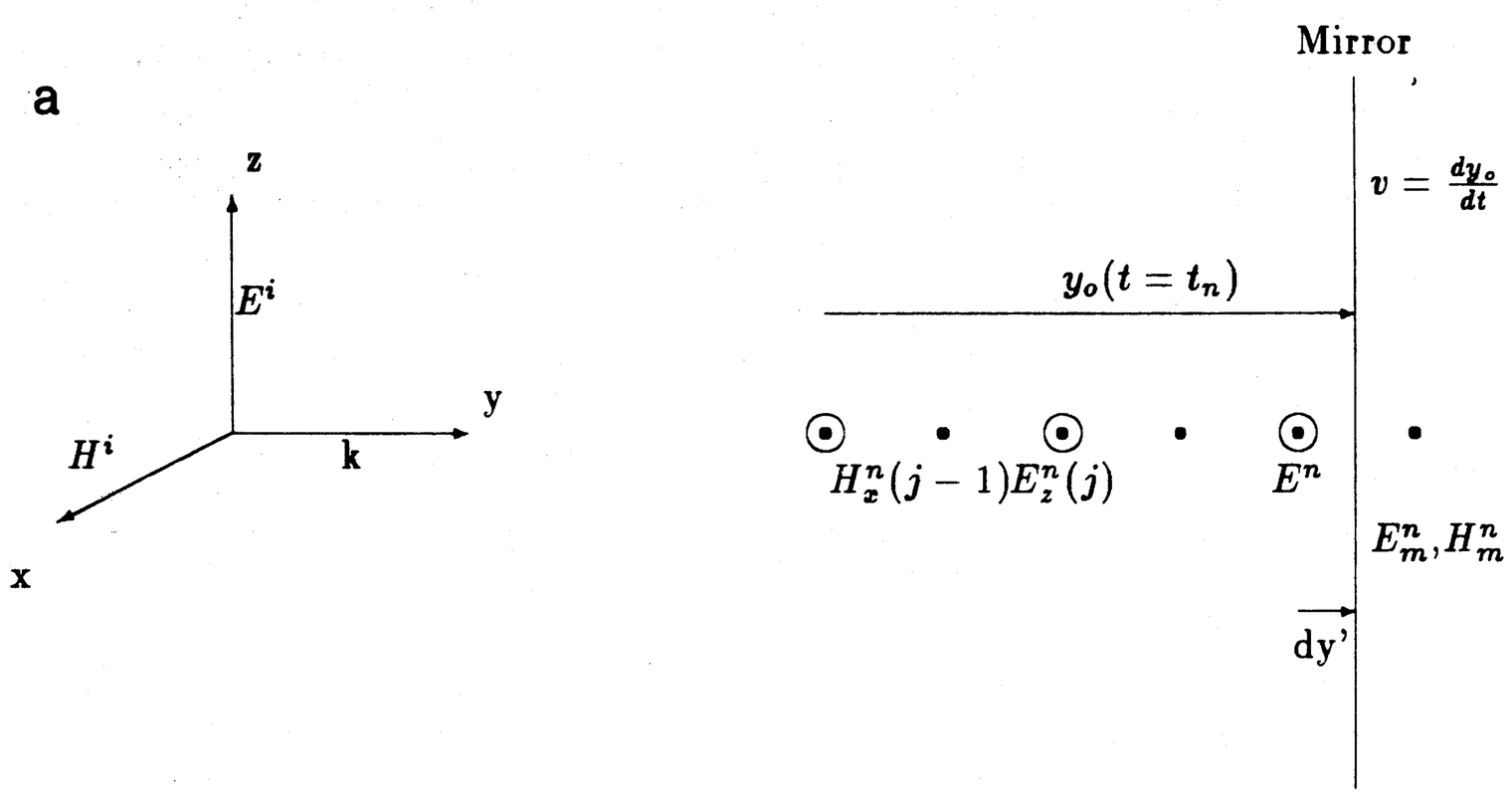

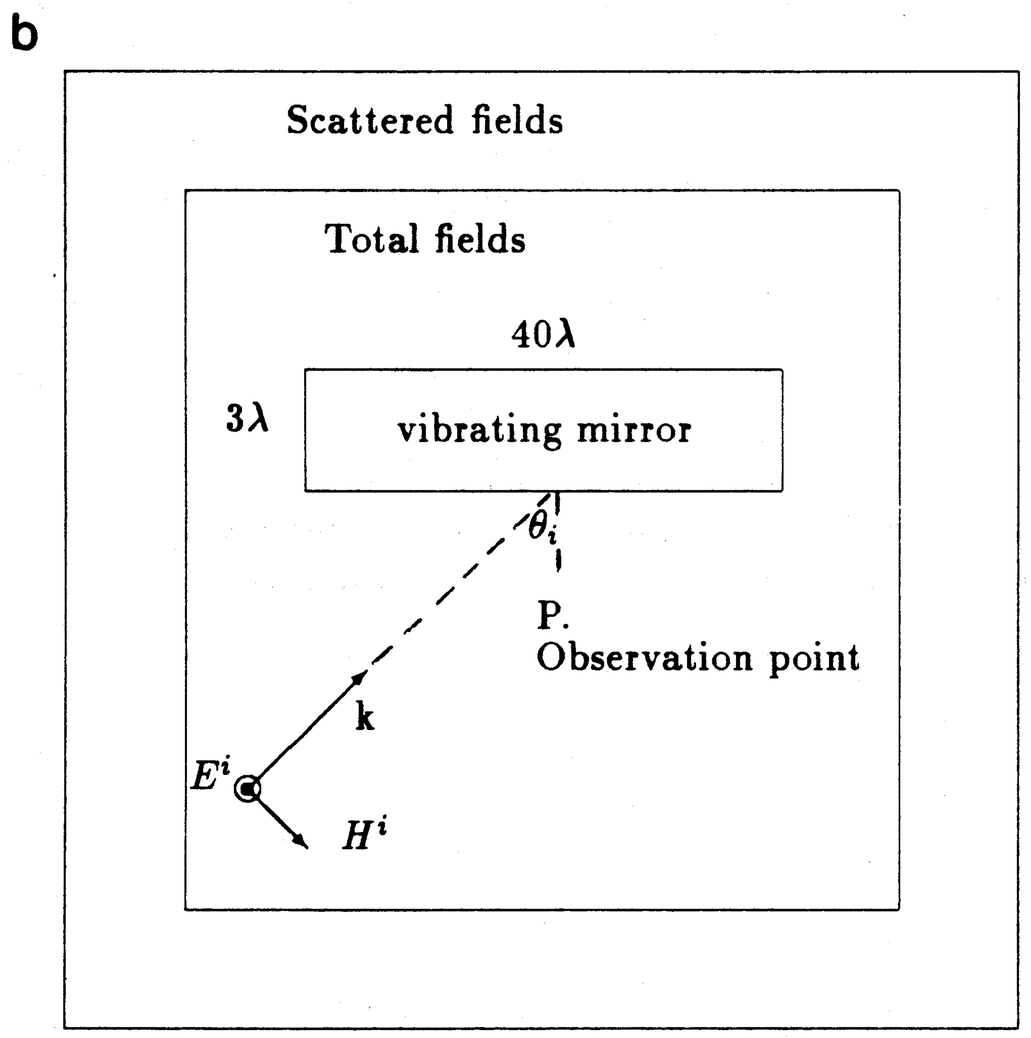

FIG. 1. (a) Snapshot of a Moving Mirror in a 1D FD-TD Grid. (b) Vibrating Mirror in a 2D FT-TD Grid.

corresponding distance from the mirror to this grid point. In all above equations (7)–(10) the mirror has a position corresponding to the time step at which the field is computed. This position, denoted by $y_0(t)$ in Fig. 1a, is computed separately in the code and is necessary to calculate dy'. Equations (7) and (8) provide us with the required field values at the mirror surface. Combining these equations with a contour integral model [14], we compute the fields adjacent to the surface. From the "co-moving" frame theory the velocity v in (1) or in (6) can be assumed to be time-varying.

3. Normal Incidence on a Moving, Infinite Conducting Sheet

3.1. *Case of a Uniform Velocity*

In our 1D model, a sinusoidal plane wave of frequency ω_i (illumination frequency) and unit amplitude is normally incident on a uniformly moving, or vibrating mirror of frequency ω_v. Referring to Fig. 1a, a positive mirror velocity, v, means that the mirror is receding from the incident wave, and a negative mirror velocity means that the mirror is advancing toward the incident wave. The scattered field from a uniformly moving mirror is given by [2]

$$E_z^r(y, t) = -\left[\frac{1-v/c}{1+v/c}\right] \exp j\left[\left(\frac{1-v/c}{1+v/c}\right)(\omega_i t - ky) + 2jk\left(\frac{r_0 - vt_0}{1-v/c}\right)\right], \quad (11)$$

where $y_0(t) = v(t-t_0) + r_0$ is the position of the mirror boundary with respect to a reference point, and r_0 and t_0 are some initial values. (For simplicity, we set both r_0 and t_0 equal to 0.) A "double-Doppler" effect is apparent from (11) in that both the frequency and amplitude of the scattered field are transformed by the same multiplying factor defined as $\alpha = (1-v/c)/(1+v/c)$.

Numerical results for double-Doppler shifts obtained with the new relativistic

TABLE I

Double-Doppler Shifts for Uniformly Moving Mirror as Obtained by FD-TD and Analysis

Velocity v	Frequency shift		Amplitude shift	
	Analytical	FD-TD	Analytical	FD-TD
$-c/3$	$2\,\omega_i$	$2\,\omega_i$	$2\,E_i$	$2.0377\,E_i$
$-c/5$	$1.5\,\omega_i$	$1.5\,\omega_i$	$1.5\,E_i$	$1.5125\,E_i$
$-c/7$	$1.33\,\omega_i$	$1.33\,\omega_i$	$1.33\,E_i$	$1.332\,E_i$
$+c/2$	$0.33\,\omega_i$	$0.33\,\omega_i$	$0.33\,E_i$	$0.329\,E_i$
$+c/3$	$0.5\,\omega_i$	$0.5\,\omega_i$	$0.5\,E_i$	$0.499\,E_i$
$+c/5$	$0.66\,\omega_i$	$0.66\,\omega_i$	$0.66\,E_i$	$0.664\,E_i$
$+c/7$	$0.75\,\omega_i$	$0.75\,\omega_i$	$0.75\,E_i$	$0.748\,E_i$

model are summarized in Table I for different approach and recession velocities. In all cases, the new model provides highly accurate results in both frequency shift and amplitude shift (within 2%).

3.2. *Case of a Sinusoidal Velocity*

For a vibrating mirror, the scattered field is given by a set of two equations [16],

$$t = t_0 + \frac{d}{c}\sin(\omega_v t_0) - \frac{y}{c} \tag{12}$$

$$E_z^r(y, t) = -\frac{1-\beta\cos(\omega_v t_0)}{1+\beta\cos(\omega_v t_0)}\cos(\omega_i t_0 - kd\sin(\omega_v t_0)), \tag{13}$$

where ω_i is the frequency of the incident wave; $y_0 = d\sin(\omega_v t)$ describes the displacement of the mirror vibrating with a frequency, ω_v and $\beta = \omega_v(d/c) = v_{\max}/c$. Equation (13) can also be written in a Fourier series expansion,

$$E_z^r(y, t) = -\mathrm{Re}\sum_{m=-\infty}^{\infty} J_{-m}(\alpha_m)\left(1+\frac{m}{m+2(\omega_i/\omega_v)}\right)e^{j(\omega_i+m\omega_v)(t+v/c)}, \tag{14}$$

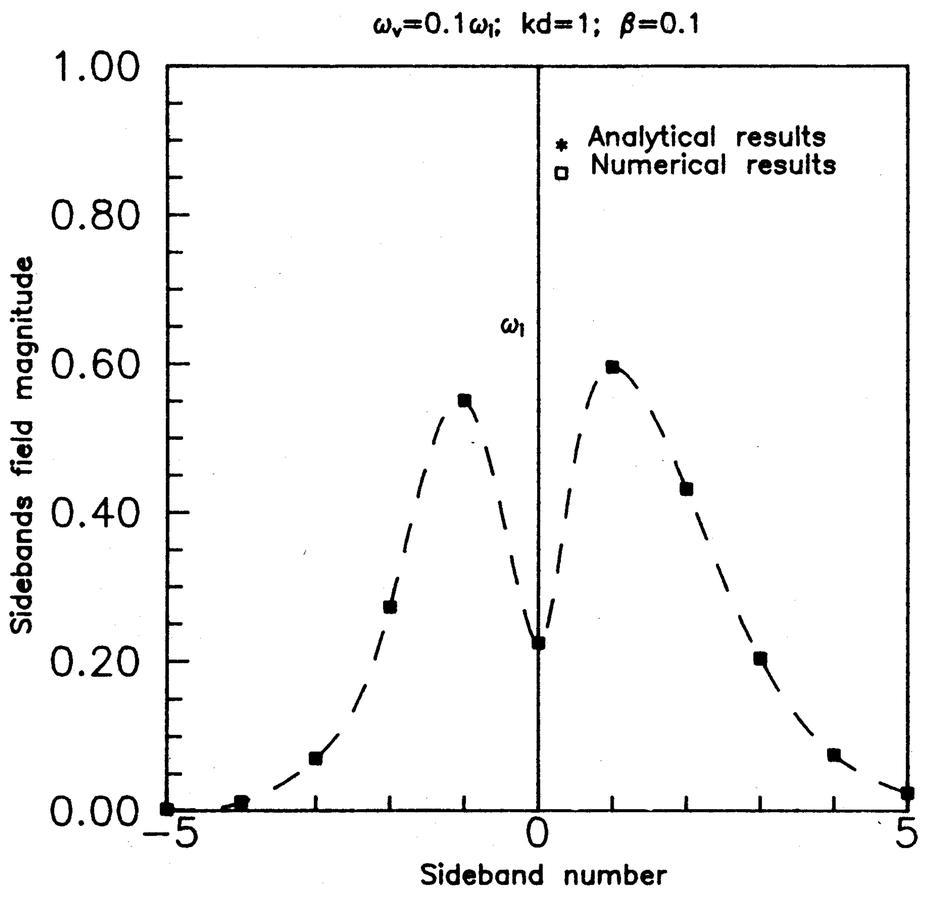

FIG. 2. Major sidebands of the reflected field spectrum as obtained both numerically and analytically.

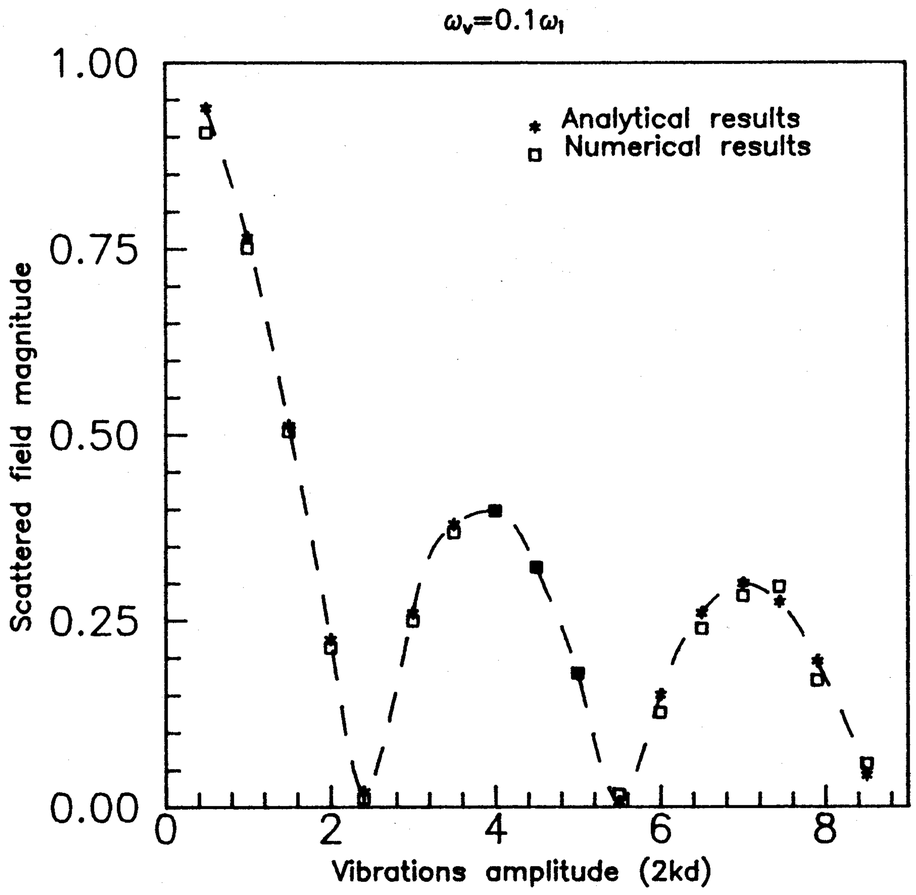

FIG. 3. Variations of the scattered field amplitude at the illumination frequency for different vibrations amplitude (d) of the mirror.

where

$$\alpha_m = m\beta + 2kd = \beta\left(m + 2\frac{\omega_i}{\omega_v}\right). \tag{15}$$

The scattered field spectrum thus contains the incident frequency ω_i and an infinity of sidebands located at $\omega_i + m\omega_v$ generated by the vibration of the mirror.

Figure 2 shows the magnitudes of the distinct sideband components of the reflected field spectrum for a mirror having a vibration frequency $\omega_v = 0.1\,\omega_i$ and $\beta = 0.1$. The spectrum is obtained by taking a discrete fast Fourier transform (FFT) of the time-domain data. To obtain a correct representation of the reflected field spectrum the sampling rate was selected such that any sideband component in the spectrum is located at exactly a discrete point. The exact values are computed using (14). The correspondence between the exact and FD-TD numerical data is so close that the stars and open squares appear as closed squares.[1] As a further test of the new model, Fig. 3 plots the variation of the scattered field amplitude at the illumination frequency for a fixed $\omega_v = 0.1\,\omega_i$ and variable β. The exact solution is obtained from (14) by setting $m = 0$ which leads to a zero-order Bessel function. Again, excellent agreement is demonstrated. Note that the model exactly detects the nulls of the Bessel function response.

[1] The dashed line is used to indicate the general shape of the spectrum and not a continuous spectrum.

4. Oblique Incidence on a Moving, Infinite Conducting Sheet

4.1. *Problem Description*

Consideration of an infinite planar conducting surface for moving-interface problems simplifies the problem because of the abscence of edge effects. Diffraction by an isolated, uniformly moving edge has been analytically considered by Tsandoulas [17] with respect to the far field. Also high and low frequency diffraction by a uniformly moving conducting strip has been considered respectively in [18, 19]. But to our knowledge, the analytical solution of an infinite vibrating strip or wedge has not yet been reported.

The model problem considered here is shown in Fig. 1b. A thin rectangular conducting slab is placed at the center of a two-dimensional FD-TD code. A plane wave strikes the surface of the slab at an oblique incident angle defined in the code. The goal here is to reconstruct published analytical results for reflection of obliquely incident waves by an infinite, vibrating, perfectly conducting planar surface, thereby validating the new numerical model. The form of the numerical relativistic equations (7) and (8) derived for the 1D problem are still valid for the 2D problem. It should be noted that the finite-size slab in the FD-TD grid introduces edge effects. To reduce or eliminate these effects via causal isolation, we obtain the early-time response for a sufficiently long slab. It is observed that as the incident angle becomes more grazing, we need to further increase the length of the slab for this purpose.

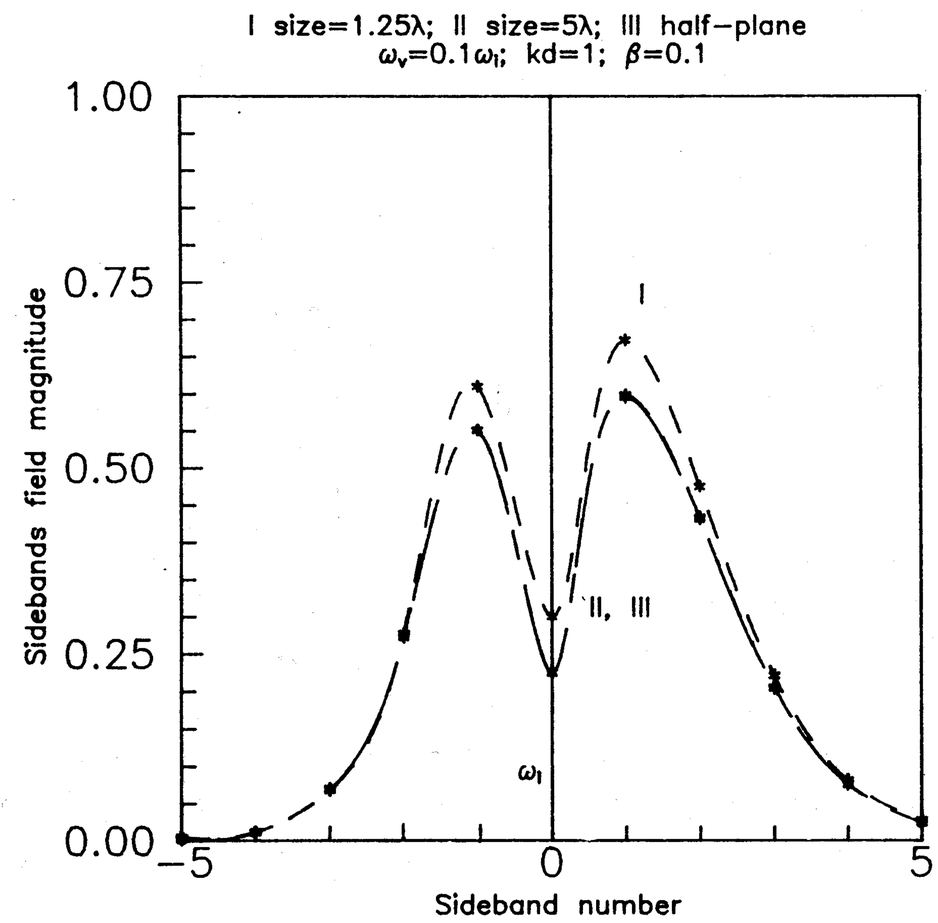

FIG. 4. Convergence of Numerical results to analytical results as the size of the cylinder approaches that of a half-plane mirror.

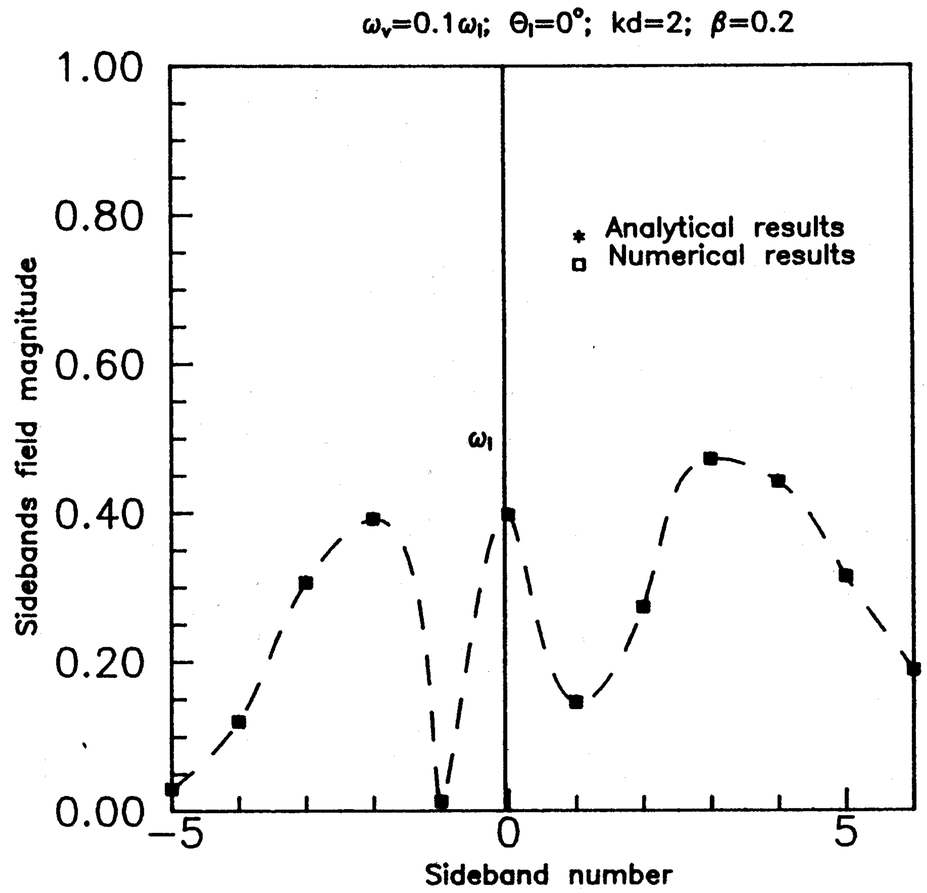

FIG. 5. Major sidebands of the reflected field spectrum as obtained both numerically and analytically.

4.2. *Comparative Results*

The first question considered is the minimum slab length necessary to approximately model an infinite mirror. Figure 4 presents an appropriate convergence study. Here, numerical data for the scattered sideband spectrum are compared to the analytical results as the length of the slab increases. The case selected is similar to the 1D case, where $kd = 0.1$, $\beta = 0.1$, and $\theta_i = 0°$. Clearly, the FD-TD results converge to the analytical results as the slab length increases from 50 cells ($1.25\,\lambda$) to 200 cells ($5\,\lambda$). The results for 100 cells ($2.5\,\lambda$), not shown here, are identical to the 200-cell results, which imply that a slab of that size is sufficiently long to simulate an infinite mirror in a bounded FD-TD grid for the normal incidence case. As will be seen below, the slab length must be increased as the angle of incidence increases, to isolate edge effects.

At oblique incidence, we have much more complicated physics because the scattered wave has a spread both in frequency and angle of reflection. The analytical solution form, described in [20], solves a set of algebraic equations given by[2]

$$\sum_{m=-\infty}^{m=\infty} jkA_m J_{n-m}(\gamma_m d) = J_{-}n(kd\cos\theta_i), \tag{16}$$

[2] Table I of [20] reports values of A_m obtained from (16) for $\theta_i = 45°$. We need to multiply each A_m term in this table by $(K+mk)/k$ to get the desired Fourier spectral components. The coefficients designated by A_m in this table are really normalized amplitudes; in other words they are really kA_m, where $k = 1$.

where

$$\gamma_m = (k + mK)\left[1 - \frac{k^2 \sin^2 \theta_i}{(k + mK)^2}\right]^{1/2} \tag{17}$$

and $K = \omega_v/c$.

To validate our method we numerically solved (16) for angles of incidence between 0° and 50° for the case $kd = 2$, and $\beta = 0.2$. Figures 5–7 are graphs of the reflected sideband spectra corresponding to these angles of incidence. For each incident angle we note that the shape of the spectrum is quite different. Yet, the numerical model provides the proper sideband structure as given by the analytical theory. It is noted that the selected size of the slab at oblique incidence is greater than for the normal incidence case to minimize edge effects. It was also noted, during our test runs, that the model is correctly sensitive to a small 5° change in the angle of incidence.

Following the analysis in [20] it can be shown that the scattered field magnitude at the illumination frequency varies closely as

$$J_0(2kd \cos \theta_i). \tag{18}$$

In Fig. 8 we have plotted the above Bessel function versus illumination angle together with the results obtained from (16) and the FD-TD model. It is clearly seen that (18) constitutes a good approximation to the series solution obtained

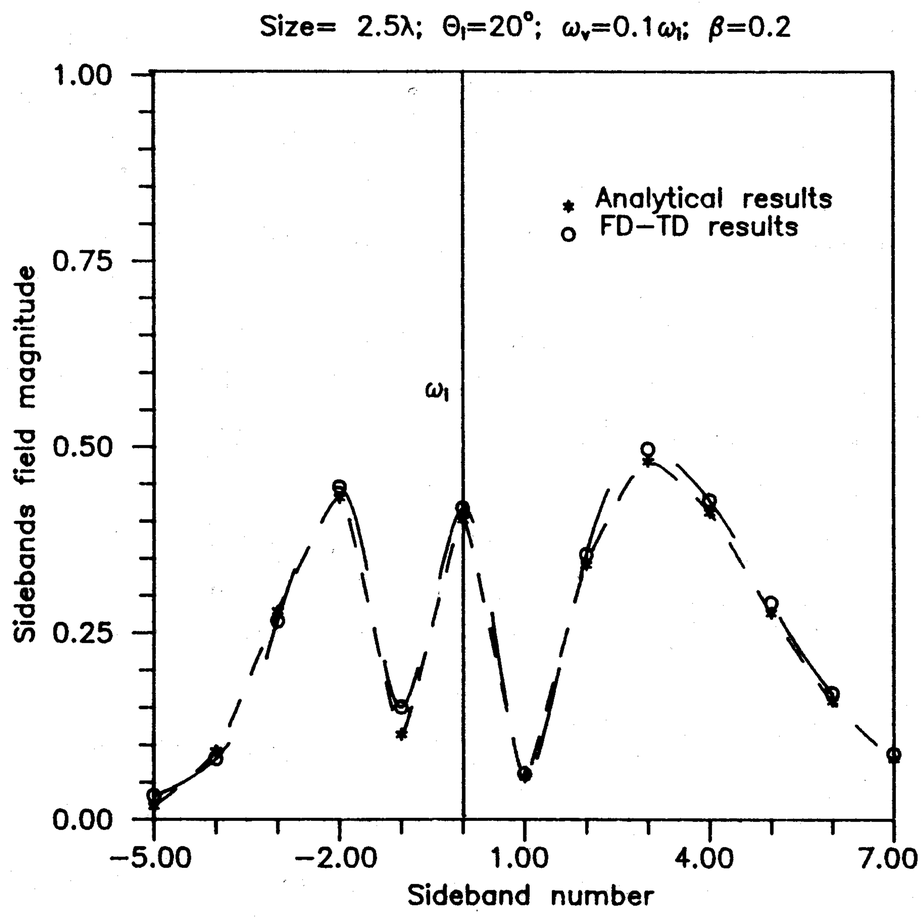

FIG. 6. Major propagating sidebands of the reflected field spectrum as obtained by FD-TD and analytically.

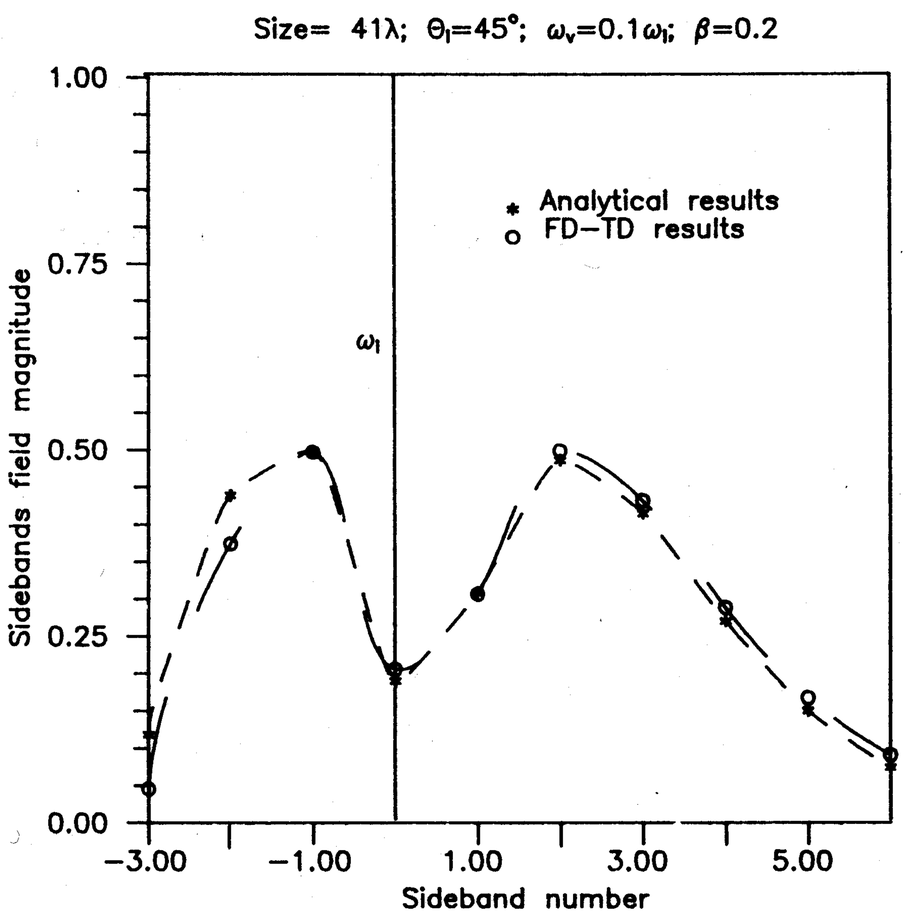

FIG. 7. Major propagating sidebands of the reflected field spectrum as obtained by FD-TD and analytically.

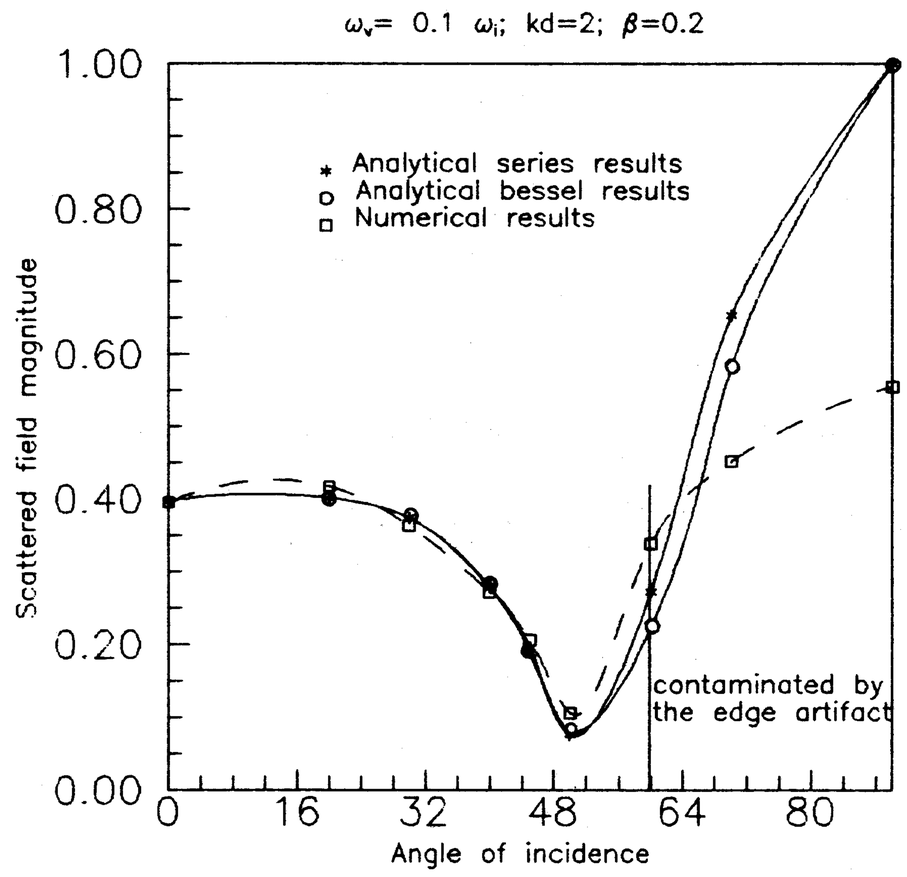

FIG. 8. Variations of the scattered field amplitude at the illumination frequency ω_i for different angles of incidence θ_i.

from (16) over the entire angular range. Also, the correspondence between analytical and numerical results is very good up to almost 60°. At larger angles, the correspondence becomes less exact because of the edge effect. The analytically predicted value of 1 at $\theta_i = 90°$ (grazing) arises because the vibration of the mirror is insensitive to the incident wave and acts like a stationary surface.

5. Summary and Conclusion

We have presented a new method to incorporate relativistic boundary conditions at the surface of a moving conductor in a 1D and 2D numerical wave propagation codes. The model proposed is an exact one which eliminates the plane-wave assumption necessary in our earlier models. Two types of relativistic mirror motion have been considered: translation and vibration. Numerical results obtained were compared against the exact analytical solution, and uniformly good agreement was demonstrated. The numerical technique reported is unique in that it requires no system transformation, contrary to other methods where the problem is first solved in the moving frame and then transformed back to the rest frame. The method can be directly adapted to model other types of relativistic moving boundary problems involving two- and three-dimensional perfectly-conducting bodies of finite size and arbitrary shape. Extension to penetrable material bodies should be feasible as well. The new method promises to be a powerful tool to model electromagnetic wave interactions with complex moving obstacles where the analysis would be virtually intractable.

Appendix

Following is the derivation of Eq. (6). We shall assume a TM wave of components (E_z, H_x, H_y). The relativistic boundary condition (1) is now written as

$$E_x = v \cdot B_x. \tag{19}$$

Assuming v to be time dependent, by total differentiating both sides we obtain

$$\frac{dB_x}{dt} = \frac{1}{v} \cdot \left(\frac{dE_z}{dt} - \frac{dv}{dt} \cdot B_x \right). \tag{20}$$

From Maxwell's equation we have

$$\frac{\partial E_z}{\partial_y} = -\frac{\partial B_x}{\partial t} \tag{21}$$

which, together with

$$\frac{dB_x}{dt} = \frac{\partial B_x}{\partial t} + v \cdot \frac{\partial B_x}{\partial y}, \tag{22}$$

lead, after simple manipulations, to

$$\mu \frac{dH_x}{dt} = \frac{v^2 - c^2}{v^2 + c^2} \cdot \frac{\partial E_z}{\partial y} - \frac{1}{v^2 + c^2} \cdot \frac{dv}{dt} \cdot E_z. \tag{A.1}$$

The term associated with $\partial B_y/\partial x$ is removed because the normal B component to the moving surface is equal to zero, from (2). Equation (A.1) corresponds to (6).

REFERENCES

1. W. PAULI, *Theory of Relativity* (Pergammon, New York, 1958).
2. J. VAN BLADEL, *Relativity and Engineering* (Springer-Verlag, New York, 1984).
3. S. L. RAY AND R. W. ZIOLKOWSKI, in *Proceedings, URSI Radio Science Meeting, Blacksburg, VA, 1987.*
4. J. VAN BLADEL, *Proc. IEEE* **64**, 301 (1976).
5. T. SHIOZAWA, *Proc. IEEE* **61**, 1694 (1973).
6. J. COOPER, *IEEE Trans. Antennas Propagat.* **AP-28**, 791 (1980).
7. K. S. YEE, *IEEE Trans. Antennas Propagat.* **AP-14**, 302 (1966).
8. A. TAFLOVE AND M. E. BRODWIN, *IEEE Trans. Microwave Theory Tech.* **MTT-23**, 623 (1975).
9. R. HOLLAND, *IEEE Trans. Nucl. Sci.* **NS-24**, 2426 (1977).
10. K. S. KUNZ AND K. M. LEE, *IEEE Trans. Electromagn. Compat.* **EMC-20**, 328 (1978).
11. D. E. MERIWETHER, R. FISHER, AND F. W. SMITH, *IEEE Trans. Nucl. Sci.* **NS-27**, 1819 (1980).
12. A. TAFLOVE, *Wave Motion* **10**, (1988).
13. F. HARFOUSH, G. A. KRIEGSMANN, AND A. TAFLOVE, in *Proceedings, URSI Radio Science Meeting, Blacksburg, VA 1987.*
14. F. HARFOUSH, A. TAFLOVE, AND G. A. KRIEGSMANN, *IEEE Trans. Antennas Propagat.* **AP-37**, (1989).
15. A. TAFLOVE, K. R. UMASHANKAR, B. BEKER, F. HARFOUSH, AND K. S. YEE, *IEEE Trans. Antennas Propagat.* **AP-36**, 1988.
16. R. E. KLEINMAN, *IEEE Trans. Antennas Propagat.* **AP-27**, 344 (1979).
17. G. N. TSANDOULAS, *Radio Sci.* **9** (1968).
18. J. D. HUNTER, *IEEE Trans. Antennas Propagat.* (1972).
19. G. N. TSANDOULAS, *J. Opt. Soc. Amer.* **59** (1969).
20. D. DE ZUTTER, *IEEE Trans. Antennas Propagat.* **AP-30**, 898 (1982).

Printed by Catherine Press, Ltd., Tempelhof 41, B-8000 Brugge, Belgium